DOI: 10.1002/ejic.200800477

Checking the Route to Cluster Helicates

Manuel R. Bermejo,*[a] Ana M. González-Noya,[b] Miguel Martínez-Calvo,[a] Rosa Pedrido,[a] María J. Romero,[a] and Miguel Vázquez López[a]

Keywords: Supramolecular chemistry / Self-assembly / Helicates / Mesocates / Cluster compounds

The aim of the work described here was to test the general applicability of our recently reported route to cluster helicates and to carry out a systematic study to relate the structural and coordinative properties of the organic strands with the microarchitectures of the resulting cluster helicates. Nine new Zn^{II}, Cu^{I} and Ag^{I} complexes were prepared from three Schiff base ligands [H_2L^a: bis(4-methyl-3-thiosemicarbazone)-2,6-diacetylpyridine; H_2L^b: bis(4-methyl-3-thiosemicarbazone)-2,6-diacetylbenzene; H_2L^c: bis(4-ethyl-3-thiosemicarbazone)-2,6-diacetylbenzene]. The experimental data confirm that Ag^{I} and Cu^{I} tetranuclear cluster helicates were obtained with a $[M_4(L^x)_2]$ stoichiometry, and this finding demonstrates the general applicability of the synthetic route. The cluster helicates presented in this work were characterized for the first time in solution by NMR spectroscopy. In addition, six of the nine complexes were characterized by X-ray diffraction studies, and three of them were found to be tetranuclear cluster helicates. A detailed study of these three crystal structures leads us to state that the changes introduced in the organic strands do not prevent the assembly of the tetranuclear cluster dihelicates, but they do affect the microarchitectures.

Introduction

In the intensive research carried out over the last ten years, hundreds of helical metallosupramolecular complexes have been reported in the literature, and several reviews on these compounds and their properties have been written.[1–4] As a result of these works, it is possible to affirm that the principles necessary for the construction of such systems are now fairly well established. However, complications associated with the simultaneous coordination of more than three metal ions with organic strands has limited most helicates to di- or trinuclear species.[5] There are some strategies for the construction of helical complexes with high nuclearity, but only a few examples of polynuclear helicates have been described in the literature.[6] In this context, we recently reported a synthetic method for the construction of a new variety of multimetallic helicates, the *cluster helicates*,[7] which we defined as *polynuclear helicates in which the metal centres are arranged forming a polyhedron around the helical axis*. The interest in this new family of supramolecular compounds results from the blend of the emerging applications of helicates[8] and the synergistic properties arising from metal ions in cluster compounds,[9] combined with the well-known advantages of the supramolecular synthetic techniques (structural control, versatility, etc.).[10] The preliminary study[7] left many unresolved issues and these included (1) the general applicability of our synthetic strategy, (2) the detailed structural characterization of the cluster helicates in solution and (3) the elucidation of the principles involved in the assembly of these supramolecular species, which would eventually allow predictive control over the microarchitectures of the final compounds.

In an attempt to address these issues, we decided to test the route to cluster helicates with ligands H_2L^a,[11a] H_2L^b and H_2L^c (Scheme 1). Our aim was to assess the applicability of the synthetic route and to carry out a systematic study in order to relate the structure and donor properties of the organic strand with the microarchitecture of the assembled cluster helicates. Herein we report the conclusions of this study.

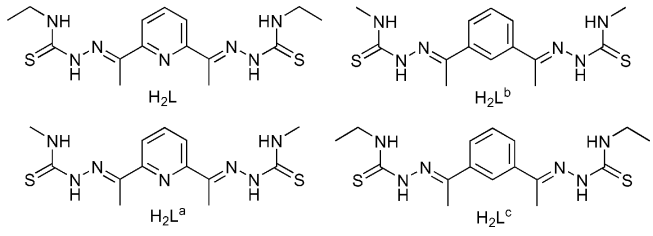

Scheme 1.

[a] Departamento de Química Inorgánica, Facultade de Química, Universidade de Santiago de Compostela, 15782 Santiago de Compostela, Spain
Fax: +34-981597525
E-mail: qimb45@usc.es
[b] Departamento de Química Inorgánica, Facultade de Ciencias, Universidade de Santiago de Compostela, 27002 Lugo, Spain
Supporting information for this article is available on the WWW under http://www.eurjic.org or from the author.

Results and Discussion

Design of the Ligands

The variety of ligands proposed, denoted H_2L^x, is illustrated in Scheme 1. Initially, we checked the route with the bis(4-methyl-3-thiosemicarbazone)-2,6-diacetylpyridine (H_2L^a) ligand.[11a] H_2L^a has the same architecture that of H_2L,[11b] with the only difference concerning the terminal alkyl chains: whereas H_2L has ethyl moieties, H_2L^a contains methyl groups. The aim of this change is to determine the way in which a less bulky terminal group influences the assembly process and the structure of the resulting "cluster helicates". In a second step, we used the bis(4-methyl-3-thiosemicarbazone)-2,6-diacetylbenzene (H_2L^b) ligand. The terminal methyl arms of H_2L^a are maintained in H_2L^b but with a very important coordinative difference: the presence of a benzene ring instead of the central pyridine spacer. Although the π-electron delocalization in both systems is similar,[12] the lone pair of electrons of the N atom makes pyridine capable of acting as a Lewis base. This fact could be of great importance, because it should affect the coordinative properties of the ligand strand in forming dihelicates, as the pyridine atom of H_2L was found to coordinate to the Zn^{II} metal centres in $[Zn_2(L_2)]$.[7] Finally, we synthesized the bis(4-ethyl-3-thiosemicarbazone)-2,6-diacetylbenzene (H_2L^c) ligand. H_2L^c maintains the terminal ethyl arms of H_2L, but it has the benzene spacer of H_2L^b.

These three ligands were synthesized by following a previously described method.[11,13] The compounds were characterized satisfactorily by elemental analysis, IR spectroscopy, mass spectrometry and ^1H and ^{13}C NMR spectroscopy (see Experimental Section).

Strategy To Generate the Metal Complexes

The first step of our strategy was the preparation of the metal(II) dinuclear dihelicate derivatives of H_2L^x. Once the ability of these ligands to form $[M_2(L^x)_2]$ helicates had been established, we proceeded to explore the possibility of increasing the nuclearity of these dinuclear species in an effort to obtain neutral dihelical compounds with a $[M_4(L^x)_2]$ stoichiometry by substituting the divalent metal centres by metal(I) ions.[7] We reasoned that if two doubly deprotonated $(L^x)^{2-}$ units are able to stabilize a neutral $[M_4(L^x)_2]$ complex, this $[M_4(L^x)_2]$ complex will have a double-helical microarchitecture, as H_2L^x is able to form dihelicates.

The zinc and silver complexes were synthesized by electrochemical oxidation of the corresponding metal anode in the presence of ligands H_2L^a, H_2L^b and H_2L^c in an organic solvent.[14] The electrochemical efficiency of the cell was close to 0.5 mol F^{-1} for the zinc complexes and close to 1.0 mol F^{-1} for the silver compounds. These values are compatible with the following reaction schemes:

Cathode: $2\ H_2L^x + 4\ e^- \rightarrow 2\ (L^x)^{2-} + 2\ H_2$

Anode: $2\ (L^x)^{2-} + 2\ Zn \rightarrow [Zn_2(L^x)_2] + 4\ e^-$

Anode: $2\ (L^x)^{2-} + 4\ Ag \rightarrow [Ag_4(L^x)_2] + 4\ e^-$

The copper(I) complexes were obtained when the ligands were treated with $[Cu(CH_3CN)_4]PF_6$ in hot acetonitrile under an argon atmosphere. In the case of the copper compound with the H_2L^a ligand, this complex could also be obtained by electrochemical synthesis. In order to avoid the oxidation of copper(I) to copper(II) a vigorous nitrogen stream was passed through the reaction mixture.

In each instance, the precipitate formed during the reaction was isolated. The solids (yellow for zinc and silver complexes, and brown for copper ones) were fully characterized by elemental analysis, IR spectroscopy, ESI mass spectrometry, conductivity measurements and magnetic moments, ^1H NMR spectroscopy and, where possible, X-ray diffraction.

The metal complexes prepared seem to be air stable in the solid state with melting points over 300 °C. Elemental analysis data (see Experimental Section) for the complexes indicate that the H_2L^x ligands (H_2L^a, H_2L^b and H_2L^c) react with zinc, copper and silver metals to afford complexes of general stoichiometry $[Zn_2(L^x)_2]$, $[Cu_4(L^x)_2]$ and $[Ag_4(L^x)_2]$, suggesting that these complexes are neutral Zn^{II}, Cu^{I} and Ag^{I} species, respectively. In these compounds, each ligand unit behaves as a doubly deprotonated system $(L^x)^{2-}$.

This formulation is also supported by molar conductivity measurements for all the complexes in 1.0 mM acetone or DMF solutions, which are in the range 2–10 Ω^{-1} cm^2 mol^{-1}, indicating the nonelectrolytic nature of these complexes.[15]

Magnetic measurements were performed at room temperature for the copper complexes. The magnetic moments of these materials are close to zero, thus confirming the +1 oxidation state for the central atom.

IR and ESI Mass Spectra

The assignments for the infrared spectra of ligands H_2L^x and their metal complexes are presented in the Experimental Section. These data support the coordination of the ligands to the metal ions. The partial deprotonation of these ligands is evidenced by the disappearance of some ν(NH) bands present in the IR spectra of the free ligands.[7,11,16] The bands corresponding to the ν(C=N) + ν(C–N) modes appear slightly shifted in all complexes, indicating coordination through the azomethine nitrogen atom.[17] The ν(C=S) bands of these ligands are slightly shifted in the spectra of the complexes, and this, together with the absence of bands due to the SH group between 2600 and 2500 cm^{-1}, indicates the coordination of the ligands to the metal centres through the thiolate sulfur atom.[18]

ESI mass spectrometry has proven to be a useful tool to investigate the presence of supramolecular species in solution.[19] In particular, this method can be useful when the powdery or poorly crystalline nature of the complexes precludes X-ray characterization. The data obtained from the ESI mass spectra are given in the Experimental Section. Copper and silver complexes show peaks assigned to the $[M_4(L^x)_2]^+$ fragments, indicating the coordination of two ligand units to the four metal centres. Furthermore, other

peaks attributable to unstable species, such as $[M(L^x)]^+$ and $[M_2(L^x)]^+$, are also present. Because the fragmentation pattern in the spectra of the $[Cu_4(L^x)_2]$ and $[Ag_4(L^x)_2]$ complexes **5**, **6** and **8** is similar to that described for **2**, **3** and **9**, which were crystallographically solved, we can suggest a tetranuclear nature for these complexes.

Peaks due to the $[M_2(L^x)_2]^+$ fragment were detected for the zinc complexes. Other minor peaks, which can be attributed to the monomeric $[M(L^x)]^+$ species, are also present. The similarities between the spectra of complexes **1**, **4** and **7** allow us to propose a dinuclear nature for these new zinc derivatives.

NMR Spectroscopy

The main signals observed in the ^1H NMR spectra of the H_2L^x ligands and their zinc, copper and silver complexes are given in the Experimental Section. With the aim of performing a comparative study, the spectrum for zinc complex **1** was recorded again. It must be noted that, in the case of the copper(I) complexes described in this paper, only the spectrum for complex **8** could be recorded, as the other complexes were found to be unstable in DMSO solutions.

Comparison of the ^1H NMR spectra of the free ligands with those of the complexes (see Figures 1, 2 and 3) allows us to highlight some general behaviour patterns for all of these systems: (1) Double deprotonation of the H_2L^x ligands in the metal complexes is evident as the amine proton signals (H_1) disappear.[20] (2) The signal due to the NH–R group (H^2) remains in the spectra of these complexes, thus confirming the double deprotonation. Moreover, the coordination of these ligands to the metal centres leads to a significant shift of these signals to higher field. The considerable upfield shift displayed by H^2 was previously observed and could be the result of strong hydrogen bonds involving the NH and thioamide nitrogen groups. (3) The influence of the coordination on the chemical shift of the aromatic proton signals is also reflected in the spectra: (i) the signal for the H^4 proton, which is located in the head of the pyridine or benzene ring, is slightly shifted; (ii) in contrast, the H^3 proton resonance shows a more marked upfield displacement in all complexes; (iii) the displacements shown by H^4 and H^3 give rise to an exchange of the relative positions of H^3 and H^4 in the case of L^a systems, as observed previously, which could be indicative of the coordination of the metal centres to the pyridine nitrogen atom;[21] (iv) in the case of complexes derived from ligands L^b and L^c, which contain benzene instead of the pyridine ring, the signal due to the H^5 proton is strongly affected by coordination and downfield displacements are observed with respect to the free ligands.

In order to obtain information that can be used as a guideline for the different behaviour of dinuclear and tetranuclear complexes in solution, some interesting findings in the zinc, copper and silver complexes spectra will be highlighted and discussed: (1) Comparison of the ^1H NMR spectra of zinc complexes with those of copper and silver

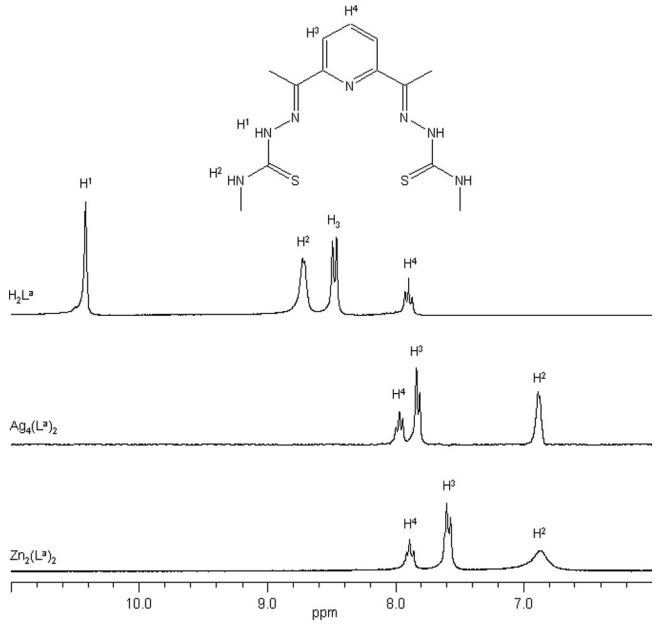

Figure 1. ^1H NMR spectra in $[D_6]$DMSO for H_2L^a and silver and zinc complexes.

systems allows us to draw very interesting conclusions: in the spectra of zinc complexes **4** and **7** (see Figures 2 and 3) the resonances due to H^2 and H^3 appear to be split, indicating that the two thiosemicarbazone arms of the ligands are not equivalent when they coordinate to both metal centres. However, the tetranuclear complexes of silver and copper only exhibit one set of signals, revealing that the two arms of the ligands are equivalent upon coordination to the metal centres. Furthermore, the spectra of silver and copper complexes are very similar, as one would expect, because both types of complexes have the same structure in the solid state. (2) Nevertheless, the spectra registered for zinc and silver complexes with ligand L^a (see Figure 1) are very similar and do not allow us to draw any conclusions, except to corroborate ligand coordination to the metal centres.

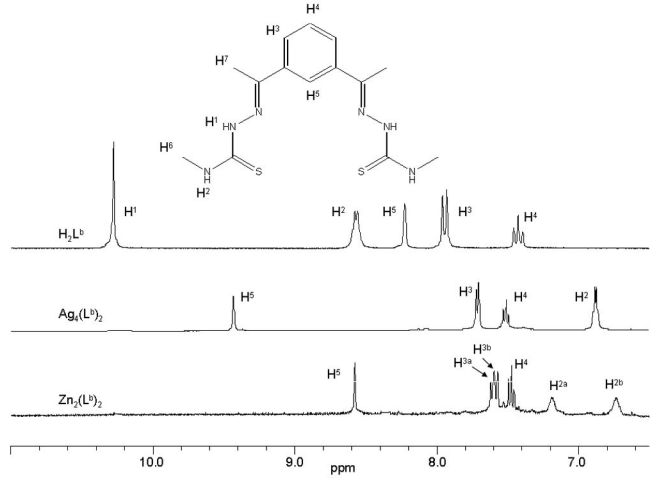

Figure 2. ^1H NMR spectra in $[D_6]$DMSO for H_2L^b and silver and zinc complexes.

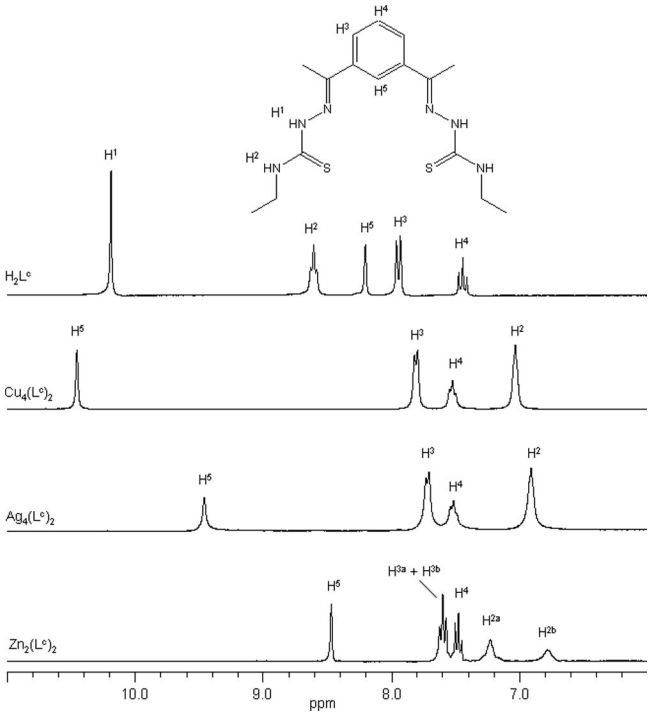

Figure 3. ^{1}H NMR spectra in [D$_6$]DMSO for H_2L^c and copper, silver and zinc complexes.

In conclusion, it seems that ^{1}H NMR spectroscopy could be a useful tool to distinguish between mesocate complexes (in the case of zinc) and tetranuclear cluster dihelicates (for copper and silver).

X-ray Diffraction Studies

Crystals of **2**, **3**, **4**, **7** and **9** suitable for study by X-ray diffraction were obtained. The most important results of the structural study for these complexes are described below.

Metal Complexes with L^a

We recently described the synthesis and structural characterization of some complexes derived from the H_2L^a ligand.[11a] In particular, we reported the crystal structure of the Zn^{II} derivative $[Zn_2(L^a)_2]\cdot EtOH\cdot 2H_2O$ (**1**; Figure 4), a common [6+4] double-stranded dinuclear helicate. The structure of **1** is very similar to that of the Zn^{II} dihelicate derived from H_2L.[7] One Zn^{II} centre is tetracoordinate in a tetrahedral mode by two imine nitrogen atoms and two thiolate sulfur atoms from two different dianionic ligand strands $(L^a)^{2-}$. The other Zn^{II} ion is hexacoordinate in a distorted octahedral mode by two pyridine nitrogen atoms, two imine nitrogen atoms, and two thiolate sulfur atoms. This coordination is achieved by symmetrical intertwining of the two ligand strands along the helical axis (Zn···Zn: 3.90 Å).

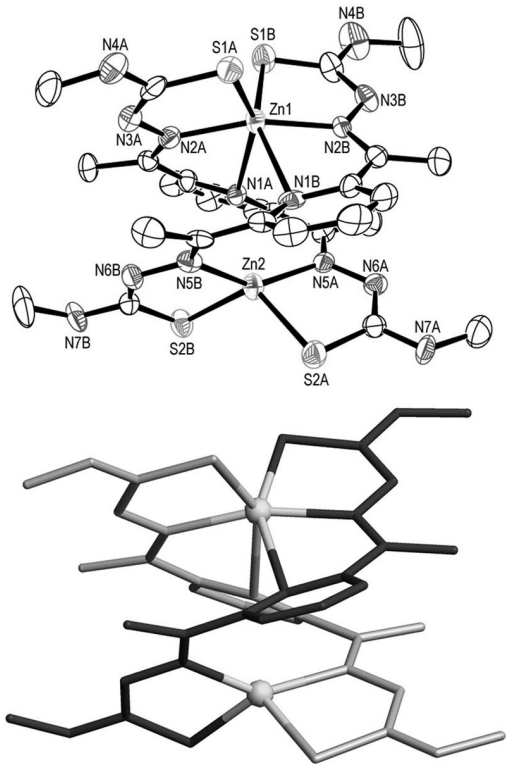

Figure 4. Top: Molecular structure of the dihelicate complex $[Zn_2(L^a)_2]\cdot EtOH\cdot 2H_2O$ (**1**),[11] with the two strands of $(L^a)^{2-}$ labelled as A and B. Thermal ellipsoids are drawn at the 40% probability level and hydrogen atoms are omitted for clarity. Bottom: Ball-and-stick representation of **1**.

It has been proven that H_2L^a has a dianionic and helicand character, and in addition, it is equipped with two soft thiolate donor atoms, which should allow the helicate assembly (dinuclear dihelical vs. tetranuclear dihelical) to be controlled through the selection of the oxidation state of the metal centres.[7,22]

Recrystallization from acetonitrile of the brown solid resulting from the synthesis of the copper(I) complex leads to single crystals of $[Cu_4(L^a)_2]\cdot 2CH_3CN$ (**2**), which were studied by X-ray diffraction. ORTEP and ball-and-stick views of **2** are shown in Figure 5. Experimental details are presented in the Experimental Section. The structure reveals the formation of the double-stranded tetranuclear cluster helicate $[Cu_4(L^a)_2]$ solvated by two molecules of CH_3CN. A racemic mixture of both enantiomers is present in the unit cell.

Each copper(I) ion is bound to one imine nitrogen atom and to two thiolate atoms, one from each ligand strand. The environment of the metal centres can be described as distorted trigonal, with both ligands acting as N_2S_2 donors. This distortion is shown by the angles between the nitrogen, copper and sulfur atoms, which range from 85.0 to 145.7°. The higher angles (143.0, 144.9, 145.3 and 145.7°) are those between copper(I), the imine nitrogen atom of one of the strands and the sulfur atom of the other. It must be noted that the pyridine donor atoms of the two $(L^a)^{2-}$ units are not involved in the coordination to the Cu^I ions.

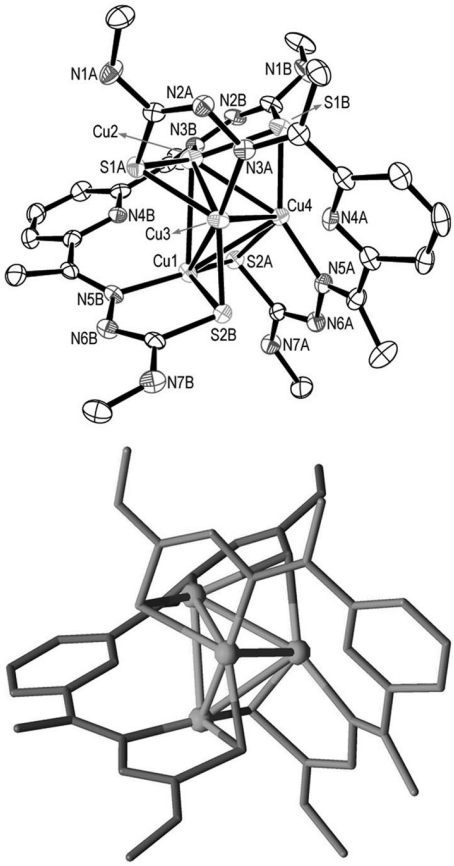

Figure 5. Top: Molecular structure of the neutral tetranuclear cluster helicate complex $[Cu_4(L^a)_2]\cdot 2CH_3CN$ (**2**), with the two strands of $(L^a)^{2-}$ labelled as A and B. Thermal ellipsoids are drawn at the 70% probability level and hydrogen atoms and solvent molecules are omitted for clarity. Bottom: Ball-and-stick representation of **2**.

A $\{Cu_4S_4\}$ cluster occupies the central part of the dihelicate, with the two $(L^a)^{2-}$ strands wrapped and intertwined around it. The cluster consists of four Cu^I ions linked together by four sulfur atoms. Each thiolate atom bridges two Cu^I ions and acts as a μ_2-donor. The dianionic nature of the ligand strands is demonstrated by the bond lengths observed for the thiourea moieties. In particular, the N_{int}–C_{thio} bond lengths (N_{int} = terminal nitrogen atom of the thiourea group; C_{thio} = carbon atom of the thiourea group), which range from 1.29 to 1.32 Å, are shorter than those found for the N_{term}–C_{thio} bonds (N_{term} = terminal nitrogen atom of the thiourea group), which range from 1.34 to 1.35 Å. In addition, the observed value for the S_{thio}–C_{thio} distances (1.76–1.77 Å) indicates the single nature of these bonds. All these data suggest a predominance of the N_{int}=C_{thio}–S_{thio} resonance form in the complex, a finding that is consistent with previous results.[7]

The intermetallic Cu···Cu distances in the $[Cu_4S_4]$ core range from 2.64 to 2.86 Å, and these are consistent with the proposed existence of Cu–Cu interactions.[23–25] Consideration of these intermetallic connections would indicate that the coordination number of the copper(I) ions should increase from 3 to 6. The four copper ions of the metallic central core define a distorted tetrahedron. This distortion is clearly revealed by the values of the Cu···Cu···Cu bond angles, which range from 56.50 to 64.84°.

The crystal structures of **2** and the Cu^I tetranuclear cluster dihelicate derived from the parent H_2L ligand ($[Cu_4(L_2)]\cdot 4CH_3CN$)[7] seem to be very similar. However, comparison of the structural information suggests that the metallic $[Cu_4]$ tetrahedron has a more compact structure in the methyl-derived cluster dihelicate **2** than in the ethyl derivative.[7] As a result, the intermetallic Cu···Cu distances oscillate from 2.64 to 2.86 Å in **2**, whereas in $[Cu_4(L_2)]\cdot 4CH_3CN$ they range from 2.67 to 2.88 Å. Moreover, the intermetallic bond angles of the central tetrahedron vary from 56.50 to 64.84° in **2**, whereas in $[Cu_4(L_2)]\cdot 4CH_3CN$ the value fluctuates from 57.16 to 65.09°. This slightly more compressed metallic core in **2** could be the result of the lower level of steric hindrance induced by the terminal methyl groups in H_2L^a with respect to the ethyl groups of H_2L, a difference that allows the ligand strands to arrange themselves more closely around the helical axis.

Once the Cu^I cluster helicate with H_2L^a had been obtained, we attempted the synthesis of the corresponding Ag^I derivative. Electrochemical oxidation[14] of a silver plate in a conducting acetonitrile solution of H_2L^a resulted in a yellow solution from which a yellow solid precipitated upon concentration under reduced pressure. Recrystallization of this solid from acetonitrile in the absence of light provided single crystals of $[Ag_4(L^a)_2]$ (**3**), which were characterized by X-ray diffraction. The crystal structure of **3** consists of an $[Ag_4S_4]$ central metallic core with two deprotonated ligand strands $(L^a)^{2-}$ wrapped around it in a helical fashion, thus forming a double-stranded tetranuclear cluster helicate. There are two different isomers of **3** in the asymmetric unit of the crystal. One of them is symmetric ($\mathbf{3}_{sym}$) and the other is asymmetric ($\mathbf{3}_{asym}$). There are four molecules of $\mathbf{3}_{asym}$ for each $\mathbf{3}_{sym}$ molecule in the unit cell. ORTEP and ball-and-stick representations of the structure of $\mathbf{3}_{asym}$ are shown in Figure 6. Moreover, ORTEP and ball-and-stick representations of the structure of the isomer $\mathbf{3}_{sym}$ can be found in the Supporting Information. Crystallographic data for **3** are presented in the Experimental Section.

Each silver(I) ion is bound to an imine nitrogen atom and a sulfur atom from one of the strands, and to a sulfur atom from the other strand. The coordination geometry of the four Ag^I ions is distorted trigonal, as shown by the observed angles between the imine, thiolate and silver atoms, which range from 75.8 to 160.4° in $\mathbf{3}_{asym}$ and from 76.2 to 159.1° in $\mathbf{3}_{sym}$. The pyridine donor atoms of the ligands remain uncoordinated.

The observed bond lengths for the thiourea moieties demonstrate the dianionic nature of the ligand strands (N_{int}–C_{thio} 1.29–1.31 Å, N_{term}–C_{thio} 1.33–1.36 Å, S_{thio}–C_{thio} 1.75–1.77 Å for $\mathbf{3}_{asym}$; N_{int}–C_{thio} 1.29 Å, N_{term}–C_{thio} 1.37 Å, S_{thio}–C_{thio} 1.75 Å for $\mathbf{3}_{sym}$) and suggest the predominance of the N_{int}=C_{thio}–S_{thio} resonance form in the complex, as found in $[Cu_4L^a_2]\cdot 2CH_3CN$.

In the $[Ag_4S_4]$ central core, each thiolate sulfur atom bridges two Ag^I ions, which are located in the vertex of a distorted tetrahedron. The Ag···Ag···Ag angles vary from

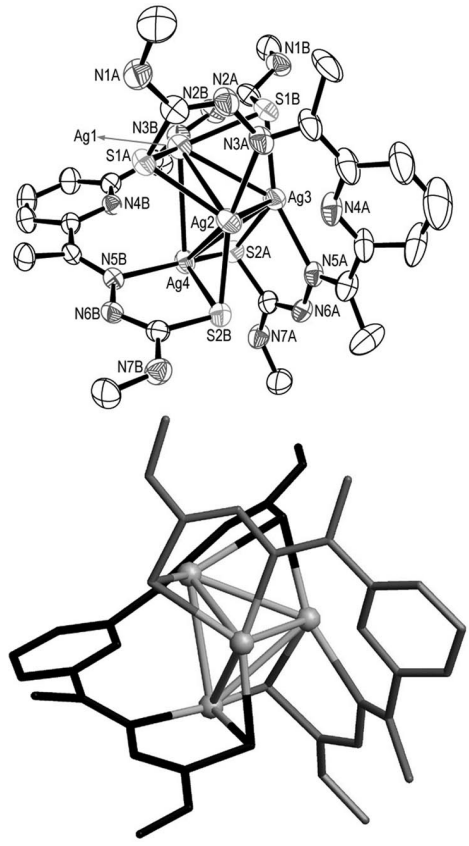

Figure 6. Top: Molecular structure of the neutral tetranuclear cluster helicate complex $[Ag_4(L^a)_2]$ ($\mathbf{3}_{asym}$), with the two strands of $(L^a)^{2-}$ labelled as A and B. Thermal ellipsoids are drawn at the 40% probability level and hydrogen atoms and solvent molecules are omitted for clarity. Bottom: Ball-and-stick representation of $\mathbf{3}_{asym}$.

57.894 to 63.243° in $\mathbf{3}_{asym}$ and from 59.344 to 61.311° in $\mathbf{3}_{sym}$. The intermetallic Ag···Ag distances range from 2.99 to 3.14 Å in $\mathbf{3}_{asym}$ and from 3.03 to 3.09 Å in $\mathbf{3}_{sym}$. These lengths are significantly shorter than the sum of the van der Waals radii for two silver atoms (van der Waals radius for Ag is 3.44 Å) and suggest the existence of metal–metal interactions.[24,26] This hypothesis implies that the coordination number of the Ag^I ions in **3** should increase from 3 to 6, which is quite unusual for this metal ion.

If we compare the intermetallic distances and angles found in the two isomers of **3** with those found in the previously reported Ag^I tetranuclear cluster dihelicate $[Ag_4L_2]$·4DMSO (Ag···Ag···Ag angles 54.74–65.41°; Ag···Ag distances 2.909–3.235 Å), it can be concluded that the metallic $[Ag_4]$ tetrahedra in $\mathbf{3}_{asym}$ and $\mathbf{3}_{sym}$ have a more compact architecture. This fact can again be explained on the basis of the lower level of steric hindrance induced by the methyl-derived H_2L^a ligand, as explained above for the Cu^I derivative with the same ligand.

Metal Complexes with L^b

The Zn^{II} derivative of this ligand was obtained electrochemically as described previously. Recrystallization of the resulting yellow solid from acetone yielded yellow crystals of $[Zn_2(L^b)_2]$ (**4**), which were analyzed by X-ray diffraction. ORTEP and ball-and-stick representations of **4** are shown in Figure 7. Experimental details are presented in the Experimental Section.

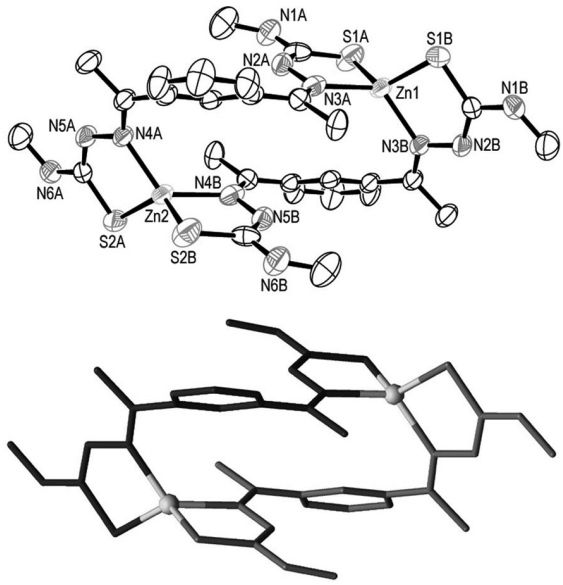

Figure 7. Top: Molecular structure of the mesocate complex $[Zn_2(L^b)_2]$ (**4**), with the two strands of $(L^b)^{2-}$ labelled as A and B. Thermal ellipsoids are drawn at the 40% probability level and hydrogen atoms are omitted for clarity. Bottom: Ball-and-stick representation of **4**.

This dinuclear Zn^{II} complex is formed by two dianionic $(L^b)^{2-}$ bridging ligands that tetrahedrally coordinate both Zn^{II} centres with distorted geometries. Two pairs of imine–thiolate donor atoms from two ligand molecules coordinate each metal centre. Both tetrahedral metal environments are heterochiral (Δ and Λ), and the ligands behave as helical threads around each metal centre. As a result, the Zn^{II} complex is achiral and thus can be termed as a *meso*-helical,[27] box-like[28] or side-by-side[29] complex, as well as a mesocate.[30] This is one of the few crystallographically characterized examples of a double-stranded *meso*-helicate described in the literature.[28,29,31] The Zn···Zn distance is 7.16 Å, almost twice the intermetallic distance found in **1**.

It seems that the pyridine nitrogen atom of the spacer determines whether the building blocks assemble into a double-stranded dihelicate or a *meso*-helical architecture. It must be noted that in [6+4] dihelicates **1** and $[Zn_2(L)_2]$,[7] the pyridine nitrogen atoms of the two ligand strands are coordinated to one of the two metal centres.

Although crystals suitable for X-ray diffraction studies could not be obtained for the $[Cu_4(L^b)_2]$ (**5**) complex, the brown solid obtained in the corresponding synthesis was identified and characterized by elemental analysis, IR spectroscopy, ESI spectrometry and magnetic and conductivity measurements (see Experimental Section).

The electrochemical synthesis of the Ag^I complex of this ligand was also carried out. The yellow solid obtained was characterized by elemental analysis, IR spectroscopy, ESI mass spectrometry, ^1H NMR spectroscopic studies and

conductivity measurements (see Experimental Section). In view of these experimental data, a formula of $[Ag_4(L^b)_2]$ (**6**) was assigned. Unfortunately, we were unable to obtain single crystals of these compounds that were appropriate for X-ray studies.

Metal Complexes with L^c

The electrochemical oxidation of a zinc plate in a conducting acetonitrile solution of the H_2L^c ligand yielded a yellow solution from which a yellow precipitate was isolated. Recrystallization of this yellow solid from acetone yielded yellow crystals of $[Zn_2(L^c)_2]\cdot 0.5(C_3H_6O)$ (**7**), which were analyzed by X-ray diffraction. ORTEP and ball-and-stick representations of the structure of **7** are shown in Figure 8. Experimental details are presented in the Experimental Section.

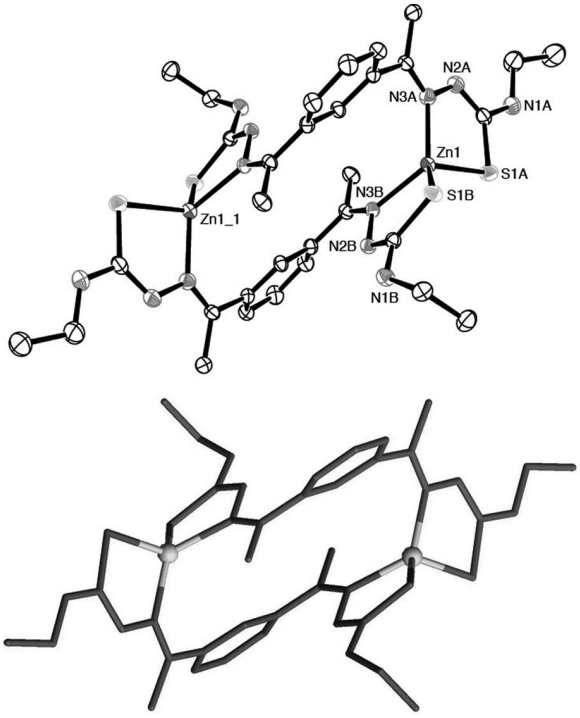

Figure 8. Top: Molecular structure of the mesocate complex $[Zn_2(L^c)_2]\cdot 0.5(C_3H_6O)$ (**7**), with the two strands of $(L^c)^{2-}$ labelled as A and B. Thermal ellipsoids are drawn at the 50% probability level and hydrogen atoms are omitted for clarity. Bottom: Ball-and-stick representation of **7**.

The structure of this achiral Zn^{II} dinuclear complex is very similar to that of complex **4**, which was discussed above. The complex is formed by two Zn^{II} ions tetrahedrally coordinated by two dianionic $(L^c)^{2-}$ ligands, both using their two pairs of imine–thiolate donor atoms in their coordination to the metal centres. Both tetrahedral metal environments are heterochiral, and so the complex can be termed as a mesocate. The Zn···Zn distance is 6.908 Å. It should be noted that the crystal cell of **7** contains another coordination isomer, where the two zinc(II) ions are coordinated to the hydrazine nitrogen atoms instead of the imine ones. A stick representation of this structure is included in the Supporting Information.

This crystal structure proves unequivocally that the presence of the pyridine nitrogen atom in the spacer in this class of ligand is crucial for the formation of Zn^{II} dihelicates.

The Cu^I complex of H_2L^c was synthesized in the usual way. The brown solid isolated after the work up of the reaction mixture was characterized by the habitual techniques (see Experimental Section) and identified as the complex $[Cu_4(L^c)_2]$ (**8**).

Finally, the electrochemical oxidation of a silver plate in a conducting acetonitrile solution of the H_2L^c ligand gave rise to a pale-yellow solution. Slow evaporation of this solution, in the absence of light, provided yellow single crystals that were isolated and identified as the compound of formula $[Ag_4(L^c)_2]$ (**9**).

ORTEP and ball-and-stick representations of **9** are shown in Figure 9. Experimental details are presented in the Experimental Section. It must be noted that the data for this crystal do not have the same level of quality as those for the other crystals reported in this work. As a result, there is some disorder in the ethyl terminal moieties of

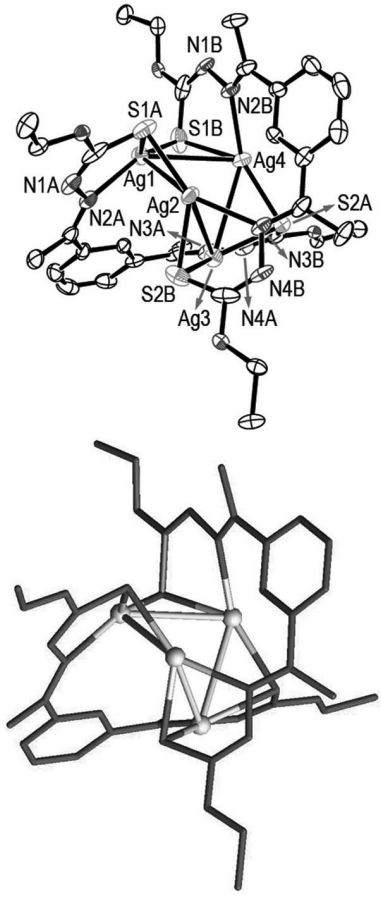

Figure 9. Top: Molecular structure of the neutral tetranuclear cluster helicate complex $[Ag_4(L^c)_2]$ (**9**), with the two strands of $(L^c)^{2-}$ labelled as A and B. Thermal ellipsoids are drawn at the 40% probability level and hydrogen atoms and solvent molecules are omitted for clarity. Bottom: Ball-and-stick representation of **9**.

the ligand, but we believe that this does not bring into question the effective formation of the tetranuclear cluster helicate or the accuracy of the bond lengths and angles found in the crystal structure.

The structure contains four Ag^I ions and two doubly deprotonated thiosemicarbazone ligands. The Ag^I centres occupy three-coordinate distorted trigonal environments, in which each metal is bound by one imine nitrogen atom and by two thiolate sulfur atoms from different ligands. Thus, both ligands act as N_2S_2 donors. All the Ag^I centres show distortion from an ideal trigonal geometry, as seen in the angles between the nitrogen, silver and sulfur atoms, which range from 78.1 to 147.7°. The four metal centres form an $[Ag_4S_4]$ central core and each thiolate sulfur atom bridges two Ag^I ions. The two ligands span the central metallic core and intertwine to give a double-helix structure. A racemic mixture of both enantiomers is observed in the unit cell.

The four Ag^I ions are located in the vertex of a distorted tetrahedron. This distortion is clearly revealed by the intermetallic bond angles and distances. The central core of the dihelicate cannot be considered a metallic tetrahedron, but rather a tetranuclear metallocycle, and the coordination number of the Ag^I ions in **9** should increase from 3 to 5. This disposition of the metallic core in **9** is quite different if we compare it with the tetrahedral metallic cores found in **3** and in the Ag^I cluster helicate derived from the $\mathbf{H_2L}$ ligand ($[Ag_4(L)_2]\cdot 4DMSO$).[7] This novel disposition of the Ag_4 central cluster is undoubtedly a consequence of the electronic change in the main body of the ligand. The substitution of the pyridine spacer by a benzene ring results in the modification of the coordination properties of the donor atoms.

Conclusions

In this work we confirm the general applicability of our route to cluster helicates.[7] We proved that some changes in the structure or in the donor properties of the organic strand H_2L,[7] such as a decrease in the steric hindrance at the terminal groups or the removal of the central pyridine nitrogen donor atom of the ligand, do not prevent the assembly of tetranuclear cluster dihelicates, but they do affect their microarchitectures. In particular, the absence of the pyridine nitrogen atom in the spacer of the organic strand leads to a novel arrangement of the central cluster core, which is a tetranuclear metallocycle instead of the common M_4 tetrahedral core. Moreover, the presence of the pyridine nitrogen donor atom in the spacer of the organic strands seems to be essential for the assembly of dinuclear dihelicates with Zn^{II} ions, as the X-ray crystal structures of the Zn^{II} derivative with H_2L^b and H_2L^c show the formation of dinuclear mesocates. However, it appears that this structural change in the organic strand does not have any consequences for the ability of H_2L^b and H_2L^c to form tetranuclear cluster helicates. In our opinion, this is because the helicand character of H_2L^b and H_2L^c remains even though they cannot form dinuclear dihelicates. All of these conclusions lead us to consider that the schematic representation of our synthetic route to cluster helicates, as described in our previous communication,[7] must be revised (Scheme 2).

Finally, it should be noted that the complexes were fully characterized in solution by NMR spectroscopy (except **2** and **5**) and ESI mass spectrometry. This is the first time that the characterization of cluster helicates has been carried out in solution. This has enabled us to correlate the behaviour

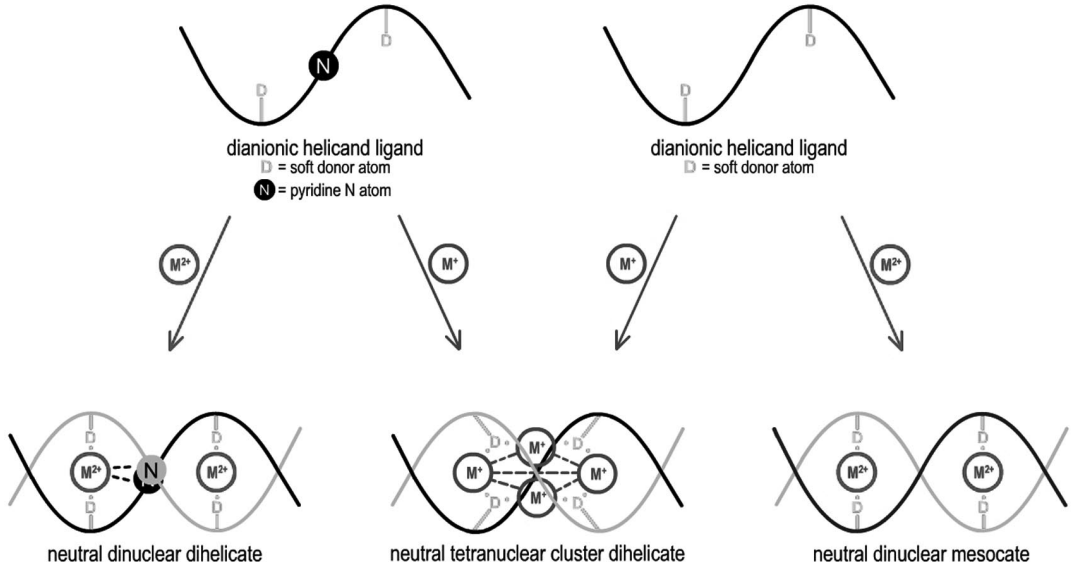

Scheme 2. "Revised" schematic representation of our synthetic approach to the assembly of "cluster helicates". The factors that make the stabilization of this new metallosupramolecular motif possible are: (i) the substitution of divalent metal centres by metal(I) ions and (ii) the presence of two soft donor atoms in the main body of a dianionic ligand, which are both able to act as terminal or bridging coordination points depending on the hardness/softness of the metal centres to which they bind.

in solution with the results found in the solid state. We are convinced that ^{1}H NMR spectroscopy will prove to be a useful tool to distinguish between dinuclear mesocates and tetranuclear cluster dihelicates.

We are currently modifying this synthetic strategy in an effort to increase the nuclearity of the resulting cluster helicates.

Experimental Section

Materials and General Methods: All starting materials were purchased from Aldrich and used without further purification. All metals were used as plates and were washed with a dilute solution of hydrochloric acid prior to the electrolysis. Elemental analyses were performed with a Carlo Erba EA 1108 analyzer. The infrared spectra were recorded from KBr pellets with a Bio-Rad FTS 175 spectrophotometer in the range 4000–600 cm^{-1}. Fast-atom bombardment (FAB) mass spectra were obtained with a Kratos MS-50 mass spectrometer by employing Xe atoms at 70 keV in *m*-nitrobenzyl alcohol as matrix. ESI spectra were obtained with an LCQDECA ion trap mass spectrometer equipped with an electrospray ionization ion source and controlled by Xcalibur software 1.1 (Thermo-Finnigan). Room-temperature magnetic susceptibilities were measured by using a Digital Measurement system MSB-MKI, calibrated by using tetrakis(isothiocyanato)cobaltate(II). Conductivity was measured at 25 °C from 10^{-3} M solutions in DMF for complexes with L^a and acetone for the remaining compounds with a CRISON Basic 30 instrument. NMR spectra were recorded with Bruker DPX-250 and AMX-500 spectrometers by using [D_6]-DMSO as solvent.

Bis(4-*N*-Methylthiosemicarbazone)-2,6-diacetylpyridine (H_2L^a): The synthesis method and the experimental data for this ligand were previously reported by us.[11a]

Bis(4-*N*-methylthiosemicarbazone)-2,6-diacetylbenzene (H_2L^b): A solution of 1,3-diacetylbenzene (0.96 g, 2.97 mmol) and 4-*N*-methylthiosemicarbazide (1.25 g, 5.94 mmol) in ethanol (125 mL) was heated under reflux for 8 h and concentrated with a Dean Stark trap to ca. 20 mL. The pale resulting yellow precipitate was collected by filtration. The solid was finally washed with diethyl ether (3 × 10 mL) and dried in vacuo. Yield: 70% (0.70 g). IR (KBr): $\tilde{\nu}$ = 3379, 3342, 3263 [ν(NH)]; 1545, 1501, 1485 [ν(C=N) + ν(C–N)]; 1113, 797 [ν(C=S)] cm^{-1}. ^{1}H NMR ([D_6]DMSO): δ = 2.34 (s, 6 H), 3.04 (d, J = 4.4 Hz, 6 H), 7.42 (t, J = 7.9 Hz, 1 H), 7.94 (d, J = 7.9 Hz, 2 H), 8.22 (s, 1 H), 8.55 (q, J = 4.4 Hz, 2 H); 10.24 (s, 2 H) ppm. ^{13}C NMR ([D_6]DMSO): δ = 14.37 (CH_3), 31.09 (CH_3), 124.54 (C_{ar}), 127.39 (C_{ar}), 128.23 (C_{ar}), 137.87 (C_{ar}), 147.67 (C=N), 178.68 (C=S) ppm. MS (FAB): m/z = 336.0 [H_2L^b + H]$^+$. $C_{14}H_{20}N_6S_2$ (336.12): calcd. C 50.0, H 5.9, N 25.0, S 19.0; found C 49.8, H 6.3, N 24.7, S 19.2.

Bis(4-*N*-ethylthiosemicarbazone)-2,6-diacetylbenzene (H_2L^c): A solution of 2,6-diacetylbenzene (1 g, 6.1 mmol) and 4-*N*-ethylthiosemicarbazide (1.4 g, 12.2 mmol) in ethanol (250 mL) was heated under reflux for 4 h and concentrated with a Dean Stark trap to ca. 20 mL and cooled over 12 h (4 °C). The yellow precipitate was filtered off, washed with diethyl ether (3 × 10 mL) and dried in vacuo. Yield: 89% (1.98 g). IR (KBr): $\tilde{\nu}$ = 3369, 3344, 3238 [ν(NH)]; 1536, 1499, 1482 [ν(C=N) + ν(C–N)], 1111, 849 [ν(C=S)] cm^{-1}. ^{1}H NMR ([D_6]DMSO): δ = 1.15 (t, J = 7.0 Hz, 6 H), 2.35 (s, 6 H), 3.64 (m, 4 H), 7.44 (t, J = 7.8 Hz, 1 H), 7.95 (d, J = 7.8 Hz, 2 H), 8.21 (s, 1 H), 8.61 (t, J = 5.7 Hz, 2 H), 10.19 (s, 2 H) ppm. ^{13}C NMR ([D_6]DMSO): δ = 14.37 (CH_3), 14.51 (CH_3), 38.43 (CH_2), 124.50 (C_{ar}), 127.37 (C_{ar}), 128.23 (C_{ar}), 137.82 (C_{ar}), 147.66 (C=N), 176.59 (C=S) ppm. MS (FAB): m/z = 365.1 [H_2L^c + H]$^+$. $C_{16}H_{24}N_6S_2$ (364.54): calcd. C 52.7, H 6.6, N 23.1, S 17.6; found C 52.9, H 6.7, N 22.8, S 17.8.

Synthesis of Complexes: The synthesis method and the experimental data for [$Zn_2(L^a)_2$]·EtOH·2H_2O (**1**) were previously reported by us.[11a] The remaining Zn^{II} and Ag^{I} complexes [$Ag_4(L^a)_2$]·H_2O (**3**), [$Zn_2(L^b)_2$] (**4**), [$Ag_4(L^b)_2$] (**6**), [$Zn_2(L^c)_2$] (**7**) and [$Ag_4(L^c)_2$] (**9**) and the copper derivative [$Cu_4(L^a)_2$]·2CH_3CN (**2**) were obtained by an electrochemical procedure.[32] The cell system can be summarized as Pt(–)/MeCN + H_2L^x/M(+), where M = Zn, Cu or Ag. The electrochemical synthesis of these complexes can be exemplified by the preparation of **4**: a suspension of ligand H_2L^b (0.1 g, 0.297 mmol) in acetonitrile (80 mL), containing tetramethylammonium perchlorate (10 mg) and with the use of a platinum wire as the cathode and a zinc plate as the anode, was electrolyzed for 1.5 h by using a current of 10 mA. (*CAUTION: Although no problems were encountered in our experiments, all perchlorate compounds are potentially explosive and should be handled in small quantities and with great care!*). The resulting yellow solid was filtered off, washed with diethyl ether and dried in vacuo. All of the electrochemically obtained metal complexes were isolated with high purity and yield.

The Cu^{I} complexes [$Cu_4(L^a)_2$]·2CH_3CN (**2**), [$Cu_4(L^b)_2$] (**5**) and [$Cu_4(L^c)_2$] (**8**) were obtained by reaction of a Cu^{I} salt with the corresponding ligand in acetonitrile and in the absence of oxygen. The synthesis of these complexes can be typified by the preparation of **2**: [$Cu(MeCN)_4$]PF_6 (204.0 mg, 0.652 mmol) was added under an argon atmosphere to a degassed solution of H_2L^a (0.1 g, 0.296 mmol) in acetonitrile (50 mL). The solution was stirred under an argon atmosphere and heated under reflux for 3 h. The solution was then concentrated under reduced pressure to give a brown precipitate. The solid was filtered off, washed with diethyl ether and hexane and dried under vacuum overnight.

Selected Data for 2: Yield: 88% (0.26 g). Λ_M = 25 Ω^{-1} cm^{2}mol^{-1}. IR (KBr): $\tilde{\nu}$ = 3314 [ν(NH)]; 1585, 1511, 1464 [ν(C=N) + ν(C–N)]; 1099, 806 [ν(C=S)] cm^{-1}. MS (ESI): m/z = 925.1 [$Cu_4(L^a)_2$ + H]$^+$, 462.9 [$Cu_2(L^a)$ + H]$^+$, 399.0 [$Cu(L^a)$ + H]$^+$. $C_{30}Cu_4H_{40}N_{16}S_4$ (1007.20): calcd. C 35.8, H 4.0, N 22.3, S 12.7; found C 35.7, H 4.2, N 22.3, S 12.7.

Selected Data for 3: Yield: 85% (0.28 g). Λ_M = 4.0 Ω^{-1} cm^{2}mol^{-1}. IR (KBr): $\tilde{\nu}$ = 3369, 3328 [ν(NH)]; 1550, 1509, 1496 [ν(C=N) + ν(C–N)]; 1110, 868, 817 [ν(C=S)] cm^{-1}. ^{1}H NMR ([D_6]DMSO): δ = 2.4 (s, 6 H), 2.7 (d, J = 4.6 Hz, 6 H), 6.9 (q, J = 4.6 Hz, 2 H), 7.8 (d, J = 7.6 Hz, 2 H), 8.0 (t, J = 7.6 Hz, 1 H) ppm. MS (ESI): m/z = 1102.8 [$Ag_4(L^a)_2$ + H]$^+$, 552.0 [$Ag_2(L^a)$ + H]$^+$, 444.0 [$Ag(L^a)$ + H]$^+$. $Ag_4C_{26}H_{34}N_{14}S_4$ (1102.38): calcd. C 28.3, H 3.1, N 17.8, S 11.6; found C 28.1, H 3.1, N 17.6, S 11.5.

Selected Data for 4: Yield: 90% (0.21 g). Λ_M = 10.0 Ω^{-1} cm^{2}mol^{-1}. IR (KBr): $\tilde{\nu}$ = 3373 [ν(NH)]; 1491 [ν(C=N) + ν(C–N)]; 1119, 795 [ν(C=S)] cm^{-1}. ^{1}H NMR ([D_6]DMSO): δ = 2.42 (s, 3 H), 2.61 (s, 3 H), 2.85 (d, J = 4.4 Hz, 6 H), 6.74 (br. s, 1 H), 7.19 (br. s, 1 H), 7.47 (t, J = 7.9 Hz, 1 H), 7.55–7.65 (m, 2 H), 8.58 (s, 1 H) ppm. MS (ESI): m/z = 799.0 [$Zn_2(L^b)_2$ + H]$^+$, 399.2 [$Zn(L^b)$ + H]$^+$. $C_{28}H_{36}N_{12}S_4Zn_2$ (799.73): calcd. C 42.1, H 4.5, N 21.0, S 16.0; found C 42.0, H 4.4, N 21.0, S 16.3.

Selected Data for 5: Yield: 80% (0.22 g). Λ_M = 9.5 Ω^{-1} cm^{2}mol^{-1}. IR (KBr): $\tilde{\nu}$ = 3369 [ν(NH)]; 1554, 1533, 1500 [ν(C=N) + ν(C–N)]; 1121, 744 [ν(C=S)] cm^{-1}. MS (ESI): m/z = 923.3 [$Cu_4(L^b)_2$ + H]$^+$, 461.0 [$Cu_2(L^b)$ + H]$^+$, 399.2 [$Cu(L^b)$ + H]$^+$. $C_{28}Cu_4H_{36}N_{12}S_4$ (923.12): calcd. C 36.4, H 3.9, N 18.2, S 13.9; found C 36.7, H 4.0, N 18.4, S 13.6.

Selected Data for 6: Yield: 84% (0.27 g). Λ_M = 10.0 Ω^{-1} cm^2 mol^{-1}. IR (KBr): $\tilde{\nu}$ = 3365 [ν(NH)]; 1562, 1514 [ν(C=N) + ν(C–N)]; 1119, 791 [ν(C=S)] cm^{-1}. ^{1}H NMR ([D$_6$]DMSO): δ = 2.45 (s, 6 H), 2.72 (d, J = 4.4 Hz, 6 H), 6.88 (q, J = 4.4 Hz, 2 H), 7.52 (t, J = 7.9 Hz, 1 H), 7.72 (d, J = 7.9 Hz, 2 H), 9.43 (s, 1 H) ppm. MS (ESI): m/z = 1100.8 [Ag$_4$(L^b)$_2$ + H]$^+$, 551.0 [Ag$_2$(L^b) + H]$^+$, 443.0 [Ag(L^b) + H]$^+$. $Ag_4C_{28}H_{36}N_{12}S_4$ (1100.41): calcd. C 30.6, H 3.3, N 15.3, S 11.7; found C 30.6, H 3.4, N 15.4, S 11.6.

Selected Data for 7: Yield: 80% (0.19 g). Λ_M = 7.4 Ω^{-1} cm^2 mol^{-1}. IR (KBr): $\tilde{\nu}$ = 3362 [ν(NH)]; 1506, 1486, 1462 [ν(C=N) + ν(C–N)]; 1121, 849 [ν(C=S)] cm^{-1}. ^{1}H NMR ([D$_6$]DMSO): δ = 0.84 (t, J = 7.1 Hz, 3 H), 1.15 (t, J = 7.1 Hz, 3 H), 2.42 (s, 3 H), 2.60 (s, 3 H), 3.28 (m, 2 H), 3.41 (m, 2 H), 6.78 (br. s, 1 H), 7.23 (br. s, 1 H), 7.48 (t, J = 7.7 Hz, 2 H), 7.66–7.55 (m, 2 H), 8.47 (s, 1 H) ppm. MS (ESI): m/z = 857.2 [Zn$_2$(L^c)$_2$ + H]$^+$, 429.2 [Zn(L^c) + H]$^+$. $C_{32}H_{44}N_{12}S_4Zn_2$ (855.84): calcd. C 44.9, H 5.2, N 19.6, S 15.0; found C 44.6, H 5.2, N 19.7, S 14.8.

Selected Data for 8: Yield: 86% (0.23 g). Λ_M = 3.2 Ω^{-1} cm^2 mol^{-1}. IR (KBr): $\tilde{\nu}$ = 3349 [ν(NH)]; 1531, 1493, 1470 [ν(C=N) + ν(C–N)]; 1092, 835 [ν(C=S)] cm^{-1}. ^{1}H NMR ([D$_6$]DMSO): δ = 1.03 (t, J = 6.6 Hz, 6 H), 2.55 (s, 6 H), 3.15 (m, 4 H), 7.04 (t, J = 5.2 Hz, 2 H), 7.52 (t, J = 6.9 Hz, 1 H), 7.80 (d, J = 6.9 Hz, 2 H), 10.46 (s, 1 H) ppm. MS (ESI): m/z = 980.0 [Cu$_4$(L^c)$_2$ + H]$^+$, 489.3 [Cu$_2$(L^c) + H]$^+$, 427.2 [Cu(L^c) + H]$^+$. $C_{32}Cu_4H_{44}N_{12}S_4$ (979.23): calcd. C 39.3, H 4.5, N 17.2, S 13.1; found C 39.0, H 4.4, N 17.4, S 13.4.

Selected Data for 9: Yield: 82% (0.26 g). Λ_M = 2.7 Ω^{-1} cm^2 mol^{-1}. IR (KBr): $\tilde{\nu}$ = 3311 [ν(NH)]; 1558, 1513, 1466 [ν(C=N)+ν(C–N)]; 1090, 810 [ν(C=S)] cm^{-1}. ^{1}H NMR ([D$_6$]DMSO): δ = 1.10 (t, J = 7.2 Hz, 6 H), 2.42 (s, 6 H), 3.19 (m, 4 H), 6.88 (t, J = 5.3 Hz, 2 H), 7.51 (t, J = 7.2 Hz, 1 H), 7.69 (d, J = 7.2 Hz, 2 H), 9.53 (s, 1 H) ppm. MS (ESI): m/z = 1156.9 [Ag$_4$(L^c)$_2$ + H]$^+$, 579.0 [Ag$_2$(L^c) + H]$^+$. $Ag_4C_{32}H_{44}N_{12}S_4$ (1156.52): calcd. C 33.2, H 3.8, N, 14.5, S 11.1; found C 33.4, H 3.6, N 14.5, S 11.4.

Crystal Structure Determinations: All crystals were obtained by recrystallization from CH_3CN (**2**, **3** and **9**) or acetone (**4** and **7**) of the solid obtained in the corresponding synthesis. Unfortunately, all attempts to obtain single crystals suitable for X-ray diffraction for the other complexes were unsuccessful. Data for **2**, **3**, **4** and **9** were collected with a Siemens Smart CCD-1000 Diffractometer whereas a Bruker APPEX CCD Diffractometer was used for **7**, all by using graphite-monochromated Mo-K_α radiation (k = 0.71073 Å) from a fine-focus sealed tube source. The computational data and reduction were obtained by using SAINT software[33] in all cases, except for **7** and **9** where APPEX2 and BRUKER XPREP[34] were used, respectively. The structures of compounds **2**, **4**, **7** and **9** were solved by SIR97[35] whereas that of **3** was solved by using DIRDIF96,[36] and all of the structures were refined by full-matrix, least-squares based on F^2 by SHELXL.[37] In all cases, an empirical absorption correction was applied by using SADABS.[38] All non-hydrogen atoms were anisotropically refined except for the disordered atoms in **9**. All hydrogen atoms were included in the model at geometrically calculated positions and refined using a riding model.

CCDC-683569, -683570, -683571, -683572 and -683573 contain the supplementary crystallographic data for this paper. These data can be obtained free of charge from the Cambridge Crystallographic Data Centre via ww.ccdc.cam.ac.uk/data_request.cif.

Data for [Cu$_4$(L^a)$_2$]·2CH$_3$CN (2): Formula: $C_{30}H_{40}Cu_4N_{16}S_4$; M = 1007.18 g mol^{-1}; crystal system: orthorhombic; space group: *Pbca*; a = 10.414(5) Å, b = 21.491(5) Å, c = 33.906(5) Å; α = 90°, β = 90°, γ = 90°, V = 7588(4) Å^3; Z = 8; μ = 2.481 mm^{-1}; reflections collected: 87790; independent reflections: 8111; R_{int} = 0.0598; $R1$, $wR2$ [$I > 2\sigma(I)$]: 0.0365, 0.0843; $R1$, $wR2$ (all data): 0.0482, 0.0884.

Data for [Ag$_4$(L^a)$_2$] (3): Formula: $C_{32.5}H_{47.5}Ag_5N_{17.5}S_5$; M = 1383.03 g mol^{-1}; crystal system: tetragonal; space group: I-4; a = 23.052(2) Å, b = 23.052(2) Å, c = 26.541(2) Å; α = 90°, β = 90°, γ = 90°; V = 14103.3(2) Å^3; Z = 8; μ = 1.543 mm^{-1}; reflections collected: 55967; independent reflections: 12957; R_{int} = 0.0387; $R1$, $wR2$ [$I > 2\sigma(I)$]: 0.0325, 0.0788; $R1$, $wR2$ (all data): 0.0459, 0.0840.

Data for [Zn$_2$(L^b)$_2$] (4): Formula: $C_{28}H_{36}N_{12}S_4Zn_2$; M = 799.75 g mol^{-1}; crystal system: orthorhombic; space group: *Pbca*; a = 14.582(2) Å, b = 15.501(2) Å, c = 16.291(2) Å; α = 90°, β = 90°, γ = 90°; V = 3682.3(9) Å^3; Z = 4; μ = 1.567 mm^{-1}; reflections collected: 28018; independent reflections: 3166; R_{int} = 0.0484; $R1$, $wR2$ [$I > 2\sigma(I)$]: 0.0629, 0.1876; $R1$, $wR2$ (all data): 0.0851, 0.2012.

Data for [Zn$_2$(L^c)$_2$]·0.5(C$_3$H$_6$O) (7): Formula: $C_{33.5}H_{47}N_{12}O_{0.5}S_4Zn_2$; M = 884.81 g mol^{-1}; crystal system: triclinic; space group: $P\bar{1}$; a = 11.2888(3) Å, b = 12.6737(4) Å, c = 14.7425(4) Å; α = 84.596(2)°, β = 81.455(2)°, γ = 75.085(2)°; V = 2012.1(1) Å^3; Z = 2; μ = 1.443 mm^{-1}; reflections collected: 54691; independent reflections: 11756; R_{int} = 0.0311; $R1$, $wR2$ [$I > 2\sigma(I)$]: 0.0383, 0.0916; $R1$, $wR2$ (all data): 0.0553, 0.0974.

Data for [Ag$_4$(L^c)$_2$] (9): Formula: $Ag_4C_{32}H_{44}N_{12}S_4$; M = 1156.55 g mol^{-1}; crystal system: tetragonal; space group: I4(1)/a; a = 15.299(3) Å, b = 15.299(3) Å, c = 17.062(6) Å; α = 90°, β = 90°, γ = 90°; V = 3993.5(18) Å^3; Z = 4; μ = 2.183 mm^{-1}; reflections collected: 15790; independent reflections: 2055; R_{int} = 0.0975; R_1w_2 [$I > 2\sigma(I)$]: 0.0658, 0.1707; R_1w_2 (all data): 0.1139, 0.1966.

Supporting Information (see footnote on the first page of this article): Ball-and-stick representation of **3**$_{asym}$; stick representation of the coordination isomer of **7**; selected bond lengths and angles of the zinc(II) dinuclear compounds, the copper(I) tetranuclear cluster compounds and the silver(I) tetranuclear cluster compounds.

Acknowledgments

We thank the Xunta de Galicia (PGIDIT06PXIB20901PR and INCITE07PXI209140ES), Ministerio de Educación y Ciencia and ERDF (EU) (CTQ2007-62485/BQU) for financial support. We also acknowledge EU COST D31 Action "Functional Helicates" (D31/0008/04). M. V. L. thanks Ministerio de Educación y Ciencia (Spain) for a "Ramón y Cajal" contract. R. P. thanks Xunta de Galicia for a "Parga Pondal" contract.

[1] a) K. Zeckert, J. Hamacek, J.-P. Rivera, S. Floquet, A. Pinto, M. Borkovec, C. Piguet, *J. Am. Chem. Soc.* **2004**, *126*, 11589–11601; b) M. Elhabiri, J. Hamacek, J.-C. Bünzli, A.-M. Albrecht-Gary, *Eur. J. Inorg. Chem.* **2004**, 51–62; c) V. Maurizot, G. Linti, I. Huc, *Chem. Commun.* **2004**, 924–925; d) L. P. Harding, J. C. Jeffery, T. Riis-Johannessen, C. R. Rice, Z. Zeng, *Chem. Commun.* **2004**, 654–655; e) B. Quinodoz, G. Labat, H. Stoeckli-Evans, A. von Zelewsky, *Inorg. Chem.* **2004**, *43*, 7994–8004; f) F. Tuna, M. R. Lees, G. J. Clarkson, M. J. Hannon, *Chem. Eur. J.* **2004**, *10*, 5737–5750; g) H. Houjou, N. Schneider, Y. Nagawa, M. Kanesato, R. Ruppert, K. Hiratani, *Eur. J. Inorg. Chem.* **2004**, 4216–4222; h) M. Albrecht, I. Janser, R. Fröhlich, *Chem. Commun.* **2005**, 157–165; i) N. W. Alcock, G. Clarkson, P. B. Glover, G. A. Lawrance, P. Moore, M. Napitupulu, *Dalton Trans.* **2005**, 518–527; j) C. J. Baylies, J. C. Jeffery, T. A. Miller, R. Moon, C. R. Rice, T. Riis-Johannessen, *Chem. Commun.* **2005**, 4158–4159; k) M. Albrecht, S. Dehn, G. Raabe,

R. Fröhlich, *Chem. Commun.* **2005**, 5690–5691; l) C. Uerpmann, J. Malina, M. Pascu, G. J. Clarkson, V. Moreno, A. Rodger, A. Grandas, M. J. Hannon, *Chem. Eur. J.* **2005**, *11*, 1750–1756.

[2] a) A. Oleksi, A. G. Blanco, R. Boer, I. Usón, J. Aymaní, A. Rodger, M. J. Hannon, M. Coll, *Angew. Chem. Int. Ed.* **2006**, *45*, 1227–1231; b) M. Albrecht, S. Dehn, R. Fröhlich, *Angew. Chem. Int. Ed.* **2006**, *45*, 2792–2794; c) J. Xu, K. N. Raymond, *Angew. Chem. Int. Ed.* **2006**, *45*, 6480–6485; d) G. Bokolinis, T. Riis-Johannessen, L. P. Harding, J. C. Jeffery, N. McLay, C. R. Rice, *Chem. Commun.* **2006**, 1980–1981; e) S. Khalid, M. J. Hannon, A. Rodger, P. M. Rodger, *Chem. Eur. J.* **2006**, *12*, 3493–3506; f) M. Hutin, C. A. Schalley, G. Bernardinelli, J. R. Nitschke, *Chem. Eur. J.* **2006**, *12*, 4069–4076; g) A. Marquis, V. Smith, J. Harrowfield, J.-M. Lehn, H. Herschbach, R. Sanvito, E. Leize-Wagner, A. Van Dorsselaer, *Chem. Eur. J.* **2006**, *12*, 5632–5641.

[3] a) E. C. Constable in *Comprehensive Supramolecular Chemistry* (Eds.: J. L. Atwood, J. E. D. Davies, J-M. Lehn, D. D. MacNicol, F. Vögtle), Pergamon, Oxford, **1996**, vol. 9, pp. 213–252; b) C. Piguet, G. Bernardinelli, G. Hopfgartner, *Chem. Rev.* **1997**, *97*, 2005–2062; c) M. Albrecht, *Chem. Rev.* **2001**, *101*, 3457–3497; d) R. M. Yeh, A. V. Davis, K. N. Raymond in *Comprehensive Coordination Chemistry II* (Eds.: J. A. McCleverty, T. J. Meyer), Elsevier Ltd., Oxford, **2004**, vol. 7, pp. 327–355; e) M. J. Hannon, L. J. Childs, *Supram. Chem.* **2004**, *16*, 7–22; f) C. Piguet, M. Borkovec, J. Hamacek, K. Zeckert, *Coord. Chem. Rev.* **2005**, *249*, 705–726.

[4] a) M. J. Hannon, C. L. Painting, N. W. Alcock, *Chem. Commun.* **1999**, 2023–2024; b) V. Berl, I. Huc, R. G. Khoury, J.-M. Lehn, *Chem. Eur. J.* **2001**, *7*, 2810–2820; c) A. Lavalette, F. Tuna, G. Clarkson, N. W. Alcock, M. J. Hannon, *Chem. Commun.* **2003**, 2666–2667; d) S. G. Telfer, R. Kuroda, *Chem. Eur. J.* **2005**, *11*, 57–68; e) S. Mizukami, H. Houjou, K. Sugaya, E. Koyama, H. Tokuhisa, T. Sasaki, M. Kanesato, *Chem. Mat.* **2005**, *17*, 50–56.

[5] J. Sanmartín, M. R. Bermejo, A. M. García-Deibe, O. Piro, E. E. Castellano, *Chem. Commun.* **1999**, 1953–1954.

[6] a) B. Hasenknopf, J.-M. Lehn, N. Boumediene, A. Dupont-Gervais, A. Van Dorsselaer, B. Kneisel, D. Fenske, *J. Am. Chem. Soc.* **1997**, *119*, 10956–10962; b) P. L. Jones, K. J. Byrom, J. C. Jeffery, J. A. McCleverty, M. D. Ward, *Chem. Commun.* **1997**, 1361–1362; c) R. W. Saalfrank, N. Löwa, S. Trummera, G. M. Sheldrick, M. Teichertb, D. Stalke, *Eur. J. Inorg. Chem.* **1998**, 559–563; d) P. N. W. Baxter, J.-M. Lehn, G. Baum, D. Fenske, *Chem. Eur. J.* **2000**, *6*, 4510–4517; e) V. Maurizot, G. Linti, I. Huc, *Chem. Commun.* **2004**, 924–925.

[7] M. R. Bermejo, A. M. González-Noya, R. Pedrido, M. J. Romero, M. Vázquez, *Angew. Chem. Int. Ed.* **2005**, *44*, 4182–4187.

[8] a) M. Elhabiri, R. Scopelliti, J.-C. Bünzli, C. Piguet, *J. Am. Chem. Soc.* **1999**, *121*, 10747–10762; b) M. J. Hannon, V. Moreno, M. J. Prieto, E. Moldrheim, E. Sletten, I. Meistermann, C. J. Isaac, K. J. Sanders, A. Rodger, *Angew. Chem. Int. Ed.* **2001**, *40*, 880–884; c) D. Kalny, M. Elhabiri, T. Moav, A. Vaskevich, I. Rubinstein, A. Shanzer, A.-M. Albrecht-Gary, *Chem. Commun.* **2002**, 1426–1427; d) V. Amendola, L. Fabbrizzi, P. Pallavicini, E. Sartirana, A. Taglietti, *Inorg. Chem.* **2003**, *42*, 1632–1633; e) C. J. Matthews, S. T. Onions, G. Morata, L. J. S. Davis, L. Heath, D. J. Price, *Angew. Chem. Int. Ed.* **2003**, *42*, 3166–3169.

[9] a) D. Gatteschi, O. Kahn, J. S. Miller, F. Palacio, *Magnetic Molecular Materials*, Reidel, Dordrecht, **1991**; b) R. D. Adams, F. A. Cotton (Eds.), *Catalysis by Di- and Polynuclear Metal Cluster Complexes*, Wiley-VCH, New York, **1998**; c) P. Braunstein, L. A. Oro, P. R. Raithby (Eds.), *Metal Clusters in Chemistry*, Wiley-VCH, New York, **1999**, vol. 1–3; d) H. A. O. Hill, P. J. Sadler, A. J. Thomson (Eds.), *Metal Sites in Proteins and Models*, Springer, **1999**, vol. 1–3.

[10] a) F. Vögtle, *Supramolecular Chemistry*, Wiley, New York, **1991**; b) J-M. Lehn, *Supramolecular Chemistry – Concepts and Perspectives*, Wiley-VCH, **1995**; c) J. L. Atwood, G. Tsoucaris, J. Lipkowsky (Eds.), *Crystallography of Supramolecular Compounds*, Springer, **1996**; d) P. D. Beer, P. A. Gale, D. K. Smith, *Supramolecular Chemistry*, OCP, Oxford University Press, **1999**; e) M. Pons, *NMR in Supramolecular Chemistry*, Springer, **1999**; f) F. T. Edermann, I. Haiduc, *Supramolecular Organometallic Chemistry*, Wiley-VCH, **1999**; g) J. W. Steed, J. L. Atwood, *Supramolecular Chemistry*, Wiley, **2000**; h) L. F. Lindoy, I. M. Atkinson, *Self-assembly in Supramolecular Systems* (Ed.: J. F. Stoddart), Royal Society of Chemistry, **2000**; i) H. Dodziuk, *Introduction to Supramolecular Chemistry*, Springer, **2002**; j) N. Yui, *Supramolecular Design for Biological Applications*, CRC Press, **2002**; k) V. Balzani, M. Venturi, A. Credi, *Molecular Level Devices and Machines: A Journey into the Nanoworld*, Wiley-VCH, **2003**; l) J. L. Atwood, J. W. Steed, *Encyclopedia of Supramolecular Chemistry*, Marcel Dekker, **2004**, vol. 1 and 2; m) A. D. Hamilton, *Functional Synthetic Receptors*, Wiley-VCH, **2005**.

[11] a) R. Pedrido, M. R. Bermejo, M. J. Romero, M. Vázquez, A. M. González-Noya, M. Maneiro, M. J. Rodríguez, M. I. Fernández, *Dalton Trans.* **2005**, 572–579; b) M. Vázquez, L. Fabbrizzi, A. Taglietti, R. Pedrido, A. M. González, M. R. Bermejo, *Angew. Chem. Int. Ed.* **2004**, *43*, 1962–1965.

[12] K. B. Wiberg, D. Nakaji, C. M. Breneman, *J. Am. Chem. Soc.* **1989**, *111*, 4178–4190.

[13] M. Vázquez, A. Taglietti, D. Gatteschi, L. Sorace, C. Sangregorio, A. M. González, M. Maneiro, R. Pedrido, M. R. Bermejo, *Chem. Commun.* **2003**, 1840–1841.

[14] M. R. Bermejo, A. M. González-Noya, M. Fondo, A. M. García-Deibe, M. Maneiro, J. Sanmartín, O. L. Hoyos, M. Watkinson, *New J. Chem.* **2000**, *24*, 235–241.

[15] W. J. Geary, *Coord. Chem. Rev.* **1971**, *7*, 81–122.

[16] M. C. Rodríguez-Argüelles, M. Belicchi Ferrari, F. Bisceglie, C. Pelizzi, G. Pelosi, S. Pinelli, M. Sassi, *J. Inorg. Biochem.* **2004**, *98*, 313–321.

[17] A. Sreekanth, M. Joseph, H.-K. Fun, M. R. Prathapachandra Kurup, *Polyhedron* **2006**, *25*, 1408–1414.

[18] M. Belicchi Ferrari, F. Bisceglie, G. Pelosi, M. Sassi, P. Tarasconi, M. Cornia, S. Capacchi, R. Albertini, S. Pinelli, *J. Inorg. Biochem.* **2002**, *90*, 113–126.

[19] H. Cheng, D. Chun-Ying, F. Chen-Jie, M. Qing-Jin, *J. Chem. Soc., Dalton Trans.* **2000**, 2419–2424.

[20] M. Fondo, A. Sousa, M. R. Bermejo, A. García-Deibe, A. Sousa-Pedrares, O. L. Hoyos, M. Helliwell, *Eur. J. Inorg. Chem.* **2002**, 703–710.

[21] R. Pedrido, M. R. Bermejo, A. M. García-Deibe, A. M. González-Noya, M. Maneiro, M. Vázquez, *Eur. J. Inorg. Chem.* **2003**, 3193–3200.

[22] a) I. Dance, *Polyhedron* **1986**, *5*, 1037–1104; b) K. L. Tang, X. L. Jin, Y. Q. Tang, *Reviews on Heteroatom Chemistry* (Ed.: S. Oae), MYU, Tokyo, **1996**, vol. 15, p. 83; c) P. Braunstein, L. A. Oro, P. R. Raithby (Eds.), *Metal Clusters in Chemistry*, Wiley-VCH, New York, **1999**, vol. 1–3; d) D. Fenske, C. Persau, S. Dehnen, C. E. Anson, *Angew. Chem. Int. Ed.* **2004**, *43*, 305–309; e) L. J. Ashfield, A. R. Cowley, J. R. Dilworth, P. S. Donnelly, *Inorg. Chem.* **2004**, *43*, 4121–4123.

[23] P. Abraham, A. G. Samuelsen, J. Chandrasekhar, *Inorg. Chem.* **1993**, *32*, 6107–6111.

[24] J. E. Huheey, E. Keiter, A. R. L. Keiter (Eds.), *Inorganic Chemistry: Principles of Structure and Reactivity*, 4th ed., Harper Collins College Publishers, New York, **1993**.

[25] a) Y. Cheng, T. J. Emge, J. G. Brennan, *Inorg. Chem.* **1996**, *35*, 7339–7344; b) M. Faulhaber, M. Driess, K. Merz, *Chem. Commun.* **1998**, 1887–1888.

[26] a) Q.-M. Wang, T. C. W. Mak, *J. Am. Chem. Soc.* **2001**, *123*, 7594–7600; b) Q.-M. Wang, T. C. W. Mak, *Chem. Commun.* **2002**, 2682–2683.

[27] a) M. Albrecht, *Chem. Soc. Rev.* **1998**, *27*, 281–288; b) E. C. Constable, M. Neuburger, L. A. Whall, M. Zehnder, *New J. Chem.* **1998**, *22*, 219–220; c) J. Xu, T. N. Parac, K. N. Ray-

mond, *Angew. Chem. Int. Ed.* **1999**, *38*, 2878–2882; d) M. Albrecht, *Chem. Eur. J.* **2000**, *6*, 3485–3489.
[28] V. Amendola, L. Fabrizzi, P. Pallavicini, *Coord. Chem. Rev.* **2001**, *216–217*, 435–448.
[29] a) A. Bilyk, M. M. Harding, P. Turner, T. W. Hambley, *J. Chem. Soc., Dalton Trans.* **1994**, 2783–2790; b) A. Bilyk, M. M. Harding, P. Turner, T. W. Hambley, *J. Chem. Soc., Dalton Trans.* **1995**, 2549–2553.
[30] R. Kramer, I. O. Fritsky, H. Pritzkow, L. A. Kovbasyuk, *J. Chem. Soc., Dalton Trans.* **2002**, 1307–1314.
[31] A. M. García-Deibe, J. Sanmartín, M. Fondo, M. Vázquez, M. R. Bermejo, *Inorg. Chim. Acta* **2004**, *357*, 2561–2569.
[32] C. Oldham, D. G. Tuck, *J. Chem. Educ.* **1982**, *59*, 420.
[33] SAINT, *Siemens Area Detector Integration Software*, Bruker AXS Inc., Madison, WI, USA, **2003**.
[34] Bruker, *APEX2*, Bruker AXS Inc., Madison, WI, USA, **2004**.
[35] A. Altomare, C. Cascarano, C. Giacovazzo, A. Guagliardi, A. G. G. Moliterni, M. C. Burla, G. Polidori, M. Camalli, R. Spagna, *SIR*97, University of Bari, Italy, **1997**.
[36] P. T. Beurskens, G. Beurskens, W. P. Bosman, R. de Gelder, S. Garcia-Granda, R. O. Gould, R. Israel, J. M. M. Smits, *The DIRDIF96 Program System*, Technical Report of the Crystallography Laboratory, University of Nijmegen, The Netherlands, **1996**.
[37] G. M. Sheldrick, *SHELX-97 (SHELXS 97 and SHELXL 97): Programs for Crystal Structure Analyses*, University of Göttingen, Germany, **1998**.
[38] G. M. Sheldrick, *SADABS: Program for Scaling and Correction of Area Detector Data*, University of Göttingen, Germany, **1996**.

Received: May 13, 2008
Published Online: July 10, 2008

